Advanced Course and Workshop on Blood Flow
BF 2005 – (pp.451–487) – Warsaw, 2005.

Vascular Model of Heat Transfer in Perfused Tissue

Maciej Stańczyk

Institute of Fundamental Technological Research
Polish Academy of Sciences
ul. Świętokrzyska 21, 00-049 Warsaw, Poland
mstan@ippt.gov.pl

The vascular model of the bio-heat transfer for soft living tissues is described, along with its numerical implementation. Main concepts of the method are discussed and the proposed approach to the number of problems is described in detail. These include: description and generation of the tissue vasculature, tissue and blood domain discretization, method for calculation of temperatures in the coupled tissue-blood system and its numerical aspects.
Alghoritms implemented in the computer programs are described and example results are presented. Various aspects of numerical and practical nature are discussed, and the conclusions are indicated with examples and comparisons of generated structures and results.
The most important assumptions made are highlighted and the possibilities of extending the presented method are indicated. Finally, the direction of further research and possibilities created by the presented method are discussed.

Key words: *bioheat equations, soft tissue modelling, vascular models*

1. Introduction

Transport of heat in living biological tissues is a very complex phenomenon. The tissue is invariably an inhomogeneous, anisotropic material and a scene for various processes influencing the heat balance. The muscle contraction is the most notable example of heat-generating process. Also there is a plethora of transport processes concerning various body fluids. These fluids convect heat between domains of the tissue and supplement the conductive mode of heat transfer.

The influence of the circulating fluid on the heat balance is most prominent in the case of soft tissue perfused with blood. The blood flows through the vessels forming a circulatory system. The heart supplies the pressure driving the blood through the branching system of vessels that get smaller and smaller in size, until they reach the level of capillaries. At that point the blood drains into the small venous vessel that drain into larger and larger vessels ultimately bringing the blood to the heart to complete the circulation.

There are numerous refinements and exceptions to the simple picture sketched above, but it is realistic enough to serve as a basis for the further considerations of the influence of blood flow on the heat transfer in tissue. The temperature of the blood as it traverses the vessels of subsequent generations is schematically depicted in Fig. 1. The most important conclusion from this figure is the fact that the temperature of the blood is significantly different from that of the tissue only when the blood is in relatively large vessels. The thermal equilibration between the tissue and the blood vessels becomes an increasingly quicker process with the decreasing vessel diameter. This fact is even more pronounced in the data presented in Table 1. In this table the basic characteristic data for different generations of vessels are given along with the *thermal equilibration length* defined as the vessel length required for the difference of temperature between the blood (in the vessel) and the surrounding tissue to drop by the factor of e.

TABLE 1. Properties of different generations of blood vessels, after [7]; x_{eq}— thermal equilibration length.

vessel	% vascular volume	avg. radius [μm]	avg. length [mm]	x_{eq} [mm]
aorta	3.30	5 000	380	190 000
large artery	6.59	1 500	200	4 000
arterial branch	5.49	500	90	300
terminal art. branch	0.55	300	8	80
arteriole	2.75	10	2	0.005
capillary	6.59	4	1.2	0.0002
venula	12.09	15	1.6	0.002
terminal vein	3.30	750	10	100
venous branch	29.67	1 200	90	300
large vein	24.18	3 000	200	5 000
vena cava	5.49	6 250	380	190 000

The facts presented in Fig. 1 and Table 1 are sometimes simplified in order to create a specific models of heat transfer. The Pennes equation assumes

that no heat transfer between blood vessels and tissue takes place until the level of capillaries is reached, the heat exchange being immediate and complete at that level (x_{eq} is large for large vessels because of their large heat content). Conversely, the Wulff model of directed perfusion assumes that blood is equilibrated thermally with tissue all the time ($x_{\mathrm{eq}} = 0$).

The models of heat transfer in perfused tissue (bio-heat equations) available in literature can be basically divided in two classes, the continuum models and the vascular models. The brief description of these is presented in the following.

1.1. Continuum Models

The continuum models describe the perfused tissue without regarding individual blood vessels, by means of a single tissue temperature. The bio-heat equation describes the balance of energy in terms of that temperature, taking into account the blood flow via additional source terms or effective conductivity. We now review three most important continuum models.

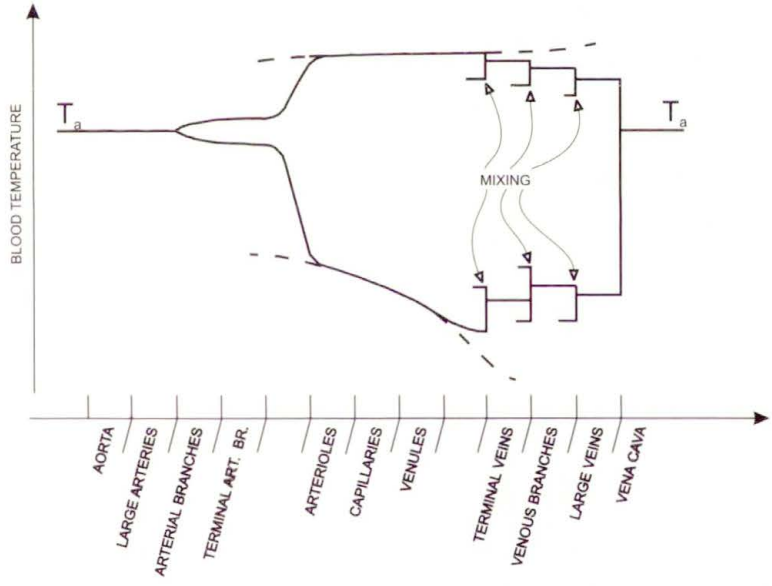

FIGURE 1. The temperature of the blood as it traverses the generations of blood vessels. The blood reaches two portions of tissue: colder than aorta blood temperature and hotter than aorta blood temperature. These two tissue temperatures are schematically indicated by the dashed line, after [7].

1.1.1. Pennes model. The Pennes model has been postulated by Harry Pennes in 1948 as a result of series of experiments aimed at measuring the temperature profile in a resting human forearm, [9]. To explain the measurement results, Pennes assumed that the essential site of blood-tissue heat exchange are capillary vessels. The blood was supposed to reach these vessels at the so-called arterial supply temperature T_{a}, and leave them at venous return temperature, which was postulated by Pennes to be equal to local tissue temperature. In the most common form, the Pennes equation also assumes that material is isotropic and material constants are independent of temperature

$$\rho c \frac{\partial T}{\partial t} = \lambda \nabla^2 T + w_{\mathrm{bl}} c_{\mathrm{bl}} (T_{\mathrm{a}} - T) + q_{\mathrm{m}} \tag{1.1}$$

where ρ and c denote tissue density and specific heat respectively, λ is tissue conductivity, w_{bl} and c_{bl} are blood perfusion rate and specific heat respectively while q_{m} is the volumetric heat source (of metabolical origin).

The most important parameter in the Pennes equation is the perfusion rate, expressed in $\mathrm{kg}_{\mathrm{blood}}$ per $\mathrm{m}^3_{\mathrm{tissue}}$ per second. It is characteristic for the given type of tissue and varies in the considerable range.

There is a vast amount of literature concerning the Pennes equation. For a detailed review the reader is referred to [12] and the references therein. The Pennes equation is undoubtedly the most popular model of bio-heat transfer and, without question, the simplest. Yet it often yields better agreement with experiments than the more elaborate models. Final remark of this brief introduction of Pennes equation: fifty years after the publication of the original paper by Pennes, Eugene Wissler critically assessed the original work of Pennes and his experimental results, [18]. Wissler concludes that the procedure adopted by Pennes was faulty and his conclusions—unfounded. Therefore it would seem that the model called by many simply "the bio-heat equation" was arrived at by chance.

1.1.2. Wulff model of directed perfusion. In 1974 Wulff raised several critical objections to the Pennes model, [19]. The most important ones were that thermal equilibration in the pre-capillary vessels should not be neglected, and that the possibly directed character of the blood flow should be taken into account.

Wulff postulated that the flow of the blood through the tissue region should be modelled in terms of the Darcy velocity $\mathbf{U}$. He also assumed that

the blood is always at the local tissue temperature. Resulting model is the usual heat conduction equation with an advective term:

$$\rho c \frac{\partial T}{\partial t} = \lambda \nabla^2 T - \rho_{\mathrm{bl}} c_{\mathrm{bl}} \mathbf{U} \cdot \nabla T + q_{\mathrm{m}}.$$

The Wulff model is not nearly as popular as Pennes equation. The assumption of instantaneous equilibration is clearly not satisfied for every vessel, cf. Fig. 1. Also blood flow is not always unidirectional, in fact this is almost never the case, and vessels most often form countercurrent pairs. For further discussion of the Wulff model the reader is referred to [12].

1.1.3. Effective conductivity models. This class of models lumps all the effects of the blood flow into an effective conductivity coefficient of the tissue. Some models assume simply that this effective tissue conductivity is proportional to first or second power of the perfusion-like parameter characterizing blood flow. The theoretical foundation for this class of models has been provided by Weinbaum and Jiji in 1985.

In the model presented in [15] they assumed that all the vessels, important to bio-heat transfer, take form of counter-current artery-vein pairs and there exists a dominant direction $\mathbf{m}$ of these pairs at every point in the tissue. They also assumed that the dominant mode of heat transfer is incomplete counter-current exchange between the vessels in the pair, and the local tissue temperature can be approximated by blood average temperature. These, and a number of other assumptions served to derive the following equation:

$$\rho c \frac{\partial T}{\partial t} = \nabla(\boldsymbol{\lambda}_{\mathrm{eff}} \nabla T) + q_{\mathrm{m}} - \frac{\pi^2 n r^2 \lambda_{\mathrm{bl}}^2}{4\sigma\lambda} \mathrm{Pe}^2 (\mathbf{m} \cdot \nabla T) \operatorname{div} \mathbf{m}$$

where n is a number density of vessel pairs in the tissue, r is the radius of a single vessel, σ is a constant shape coefficient of heat transfer and Pe is the Péclet number of blood flow in the vessel. For a detailed derivation of the equation and definition of the quantities involved, the reader is referred to the original paper [15]. The quantity $\boldsymbol{\lambda}_{\mathrm{eff}}$ is the effective conductivity tensor and is defined by

$$\boldsymbol{\lambda}_{\mathrm{eff}} = \lambda \left(\mathbf{I} + \frac{n\pi^2 r^2 \lambda_{\mathrm{bl}} \mathrm{Pe}}{4\sigma\lambda} \mathbf{m} \otimes \mathbf{m} \right)$$

where $\otimes$ denotes tensor product.

The introduction of Weinbaum-Jiji model has initiated a long-lasting discussion about the validity of the most important assumptions used. In their later paper, Weinbaum and Jiji suggest that the areas of applicability of their model are restricted to a range of vessel diameters and proposed a suitable criterion, [16], see also [6]. For more complete review of the objections raised against the Weinbaum-Jiji model and the remedies proposed, the reader is referred to [12].

1.2. Vascular Models

Vascular models describe the process of heat transfer between the blood in vessels, characterized by blood temperature and the tissue characterized by the tissue temperature. No assumption is made a priori concerning the possible equality of these two temperatures. Therefore the full range of the thermal equilibration regimes, as depicted in the Fig. 1, can be reproduced. This means however that the model needs to include the detailed information about the structure of the circulatory system within the region of interest and needs to keep track of all the blood temperatures throughout this system in order to calculate the tissue temperature.

This high level of complexity results also in high computational power needed to perform calculations on such models. In fact, the vascular model presented by Brinck and Werner in [5] could only be formulated and solved for very small region of tissue. For this reason the vascular models are not common in the literature and the only one attempt of actual calculation, known to the present author is the one presented in [5].

However, in addition to tissue temperature, it allows one to calculate all the blood temperatures and model various physiological phenomena such as vasodilation and vasoconstriction, blood viscosity changes etc. in the most straightforward manner.

The actual formulation of the vascular model developed by the author and its numerical implementation is the main topic of the present paper.

2. Method

We develop an implementation of the vascular model for calculating heat exchange in vascularized, living tissue, under prescribed heat loading conditions. The model contains a description of the complex blood circulation system occupying the tissue region of interest. It is assumed that the blood

travels through vessels that form a *tree-like structure*. The tree consists of a number of interconnected *segments*. Each segment is composed of two *vessels* lying in the counter-current arrangement. One of the vessels is the feeding vessel (artery), the other is the draining vessel (vein). Such an arrangement is found in a majority of blood vessels, [15]. The exceptions are the largest vessels (aorta and vena cava) and capillaries. When the tissue domain of interest does not contain the largest vessels (and this is the case in peripheral circulation, which is most interesting here), the former exception does not apply. Furthermore, as was shown in the preceding section, in usual thermal loading conditions, the temperature equilibration between the blood vessels and the surrounding tissue, takes place long before the blood reaches capillaries. It is hypothesized here, that this will hold true, even in the most extreme thermal loading scenarios.

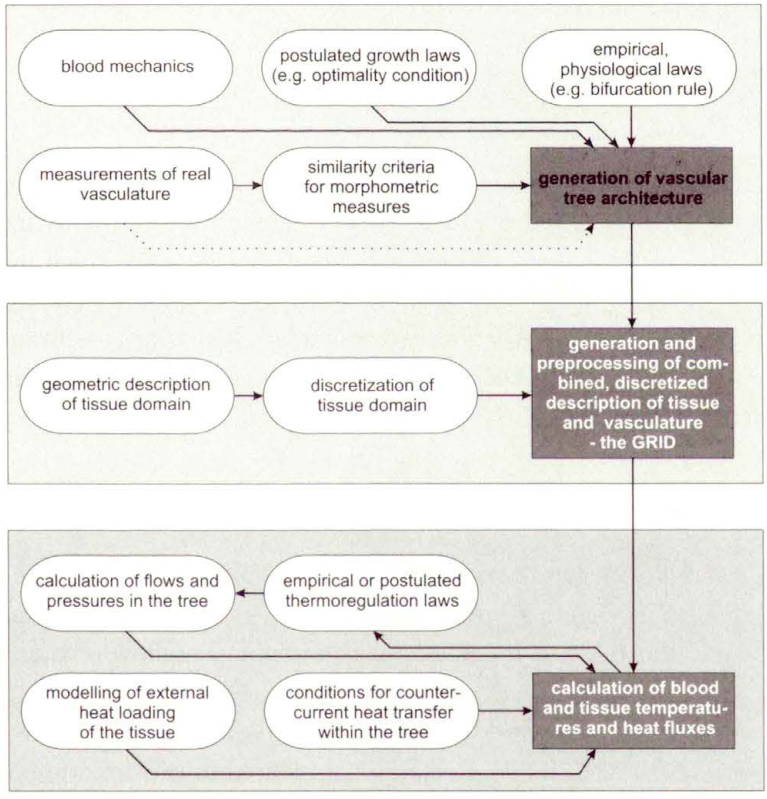

FIGURE 2. The three basic steps employed in the presented method. They are implemented in the three independent computer programs.

If we furthermore assume, that the capillaries and other smallest vessels are isotropic in their spatial arrangement, it becomes clear that the vascular model needs to include detailed description of the architecture of only those vessels that are not in the thermal equilibrium with tissue. Depending on the severity of the thermal loading to which the tissue region is subjected, different levels of detail will be needed (in the presence of steep gradients of tissue temperature, the temperatures in small arterioles and venules need to be calculated, whereas if the tissue temperature is more uniform, these temperatures may be safely assumed equal to tissue temperature).

The architecture of the realistic vascular system is reconstructed according to a number of rules. Then the tissue domain, in which the vascular tree is embedded is discretized and the relation between this discretization and the description of vasculature is established. Finally the heat exchange in various pre-defined scenarios can be calculated. In Fig. 2, the basic steps of the method are depicted.

3. Tree Generation

Generation of the vascular tree is performed by means of the algorithm based on the one presented in [10]. It aims at generation of the hydraulically balanced tree, which obeys additional *bifurcation rule*, and which minimizes the volume of blood needed to vascularize the given domain. The algorithm is a sequential one and consists of extending the existing tree branch after branch. Before we pass to the description of the algorithm let us introduce the relevant notions.

3.1. Notations

vessel—a single conduit embedded in the domain of interest (be it two- or three-dimensional), characterized by the starting and ending point, which determine the local axis of the vessel. The flow of blood in the model can take place through the vessels only. The vessel is the simplest, one-dimensional domain. Several scalar fields are defined on the vessel: vessel radius, blood velocity (measured in the direction of the local axis of the vessel) and temperature. In the method described in the present paper, both the blood velocity and vessel radius are assumed constant along the vessel.

segment—a pair of vessels, characterized by common starting and ending points, identical radii and opposite blood flow velocities. The segment is the basic building block of the vascular tree and it serves to model a counter-current artery-vein vessel pair. The vessel with positive velocity is referred to as *artery* or the *feeding vessel*, while the vessel with negative velocity is the *vein* (the draining vessel).

connected segments—two or more segments, arranged spatially in such a way, that the end-point of one of them (the *parent segment*)) is the start-point of all the others (the *daughter segments*). In the presented model it is assumed, that the blood leaving the artery of the parent segment enters the arteries of the daughter segments, also the blood leaving the veins of the daughter segments is collected in the vein of the parent segment.

bifurcation—the point, where two (or more) segments meet. The bifurcation is the end-point of one parent segment and start-point of one or more daughter segments (the bifurcation can be also called the *junction.*)

terminal segment—the segment which has no daughter segments. In the model it is assumed that the blood leaving the artery of the terminal segment enters directly the draining vessel of that segment (the vein). The temperature of this blood is assumed to change to the local tissue temperature upon entering the vein of the terminal segment. Terminal segments are designed to model the ultimate blood-tissue equilibration process in the capillaries.

root segment—the segment which has no parent segment. The temperature of the blood entering the feeding vessel of the root segment and its flow (or pressure) are prescribed boundary conditions to the model, while the temperature of the blood leaving the draining vessel of the root segment is one of the most important results from the model.

vascular tree—a system of interconnected segments, stemming from one root segment and bifurcating through a number of generations. The sequence of bifurcations ends at the terminal segments. In the presented method the generated vascular tree is initially (i.e. before it is processed for further calculations) a binary tree i.e. each non-terminal vessel has exactly two daughter vessels.

subtree—a tree formed by all descendant segments of a particular parent segment.

mesh—a discretization of tissue domain of interest into appropriate elements (for further use in finite differences, finite elements or other methods).

grid—a combined and mutually compatible discretizations of the tissue domain (the mesh) and of the vascular tree into appropriate elements and interconnected segments, supplemented with additional membership information; suitable for further calculation of coupled tissue and blood temperatures. The notion of grid is explained in detail in Sec. 4.

3.2. Generation Algorithm

The generation algorithm employed is based on the one introduced in [10]. The modifications introduced by the present author will be indicated at the end of the presentation.

It is assumed that the tissue receives the nutrients from the blood on the capillary level, which corresponds to the terminal segment in the presented model. It is furthermore assumed that exists an elementary quantity of tissue (terminal area in 2D setting or terminal volume in 3D setting), whose demand is satisfied by prescribed, elementary blood flow Q_{term} through the single terminal segment. The generation consists basically of the following steps:

1. scale the tissue region of interest until it has the elementary area or volume,
2. plant the single root terminal vessel with the start point on the boundary and end point inside this scaled region,
3. scale the tissue region, so its area/volume can accommodate one more terminal area/volume; the region needs now one more terminal segment to satisfy its demands,
4. add a new terminal segment to the tree,
5. check if a desired tissue region size/tree complexity has been attained, if not—proceed to the step (3).

Each time, before step (3) is entered, and at the end of the whole procedure, the tree complies with all the assumptions. All steps of the above algorithm, except the step (4) are simple and require no further explanations.

Step (4)—the procedure of adding the new terminal segment to the tree—is executed by means of the following algorithm:

(4.1) find a satisfactory location for the end point of prospective, new terminal segment,

(4.2) find the best segment to act as a parent segment to the new terminal,

(4.3) create the new terminal segment temporarily connecting the arbitrary point on the parent segment (the present implementation uses the point in the geometric center of the parent segment) with the end-point chosen in step (4.1),

(4.4) adjust segment radii throughout the tree to adjust the hydraulic resistance to the increased blood flow, and optimize the location of the bifurcation point based on minimization of corresponding blood volume.

We begin the detailed description of these steps with explanation of step (4.3) and (4.4). The disturbed order of the presentation is motivated by the fact that some of the preceding steps can be easily described in terms of the functionality of these steps.

3.2.1. Adding a new terminal segment to the vascular tree. The method presented in [10] (and adopted here) assumes that there are two laws, governing the sizes of the blood vessels in the vascular tree. The first is that the hydraulic balance must be achieved, i.e. the flow and pressure at the end point of each terminal vessel must be the same. This means that the ratio of total hydraulic resistances of two subtrees in the tree is inversely proportional to the ratio of the number of terminal segments in those subtrees. The hydraulic resistance of the single vessel is calculated according to the Hagen-Poiseulle law:

$$R = \frac{8\nu L}{\pi r^4}$$

where ν is blood viscosity, L is the length of the segment and r is its radius. The hydraulic resistance of the binary subtree, where the segment S is a root segment is:

$$R(S) = \begin{cases} \frac{8\nu L(S)}{\pi r^4(S)} & \text{if } S \text{ is a terminal segment,} \\ \\ \frac{8\nu L(S)}{\pi r^4(S)} + \frac{R(S_L)R(S_R)}{R(S_R)+R(S_L)} \end{cases}$$

where the notation S_L and S_R has been used to denote both daughter segments of the segment S.

The second law governing the growth of the modeled vascular tree is the bifurcation law. It is an empirical, physiological law, [10]

$$r^{\gamma}(S) = r^{\gamma}(S_L) + r^{\gamma}(S_R) \tag{3.1}$$

where γ is the prescribed *bifurcation exponent*, which is assumed to be 2.7 [10].

Equation (3.1) is known in the literature as the Murray's law. It is based on the hypothesis that the bifurcations in the vasculature are designed in such a way as to minimize the pumping power required and metabolic energy expense to drive and maintain the system [11]. It has also been proved that, this condition is equivalent to ensuring that the wall shear stress is homogeneous throughout the vascular system, [11, 13]. This latter fact is important because it gives clue to the mechanism of growth of blood vessels.

Value of the exponent γ obtained by means of theoretical study is three. Its derivation is based on several assumpions, among others of laminar blood flow obeying the Hagen-Poiseuille law and constant blood viscosity. Estimation of the γ exponent for the cases where these assumptions are relaxed yields only slight decrease in its value [11].

The optimality condition used as a starting point for construction of the transport systems (where fluid, heat, or other media is transported) underlies the so-called constructal theory, developed by A. Bejan in late 1990's [3]. While it is based on universal concepts, the constructal theory finds applications in the modelling of vascular systems [4]. The theoretical considerations of optimality lead to numerous quantitative scaling laws which are satisfied by the actual living organisms in surprisingly wide range of scales [17].

In the presented model both the hydraulic balance law and bifurcation rule are sufficient to determine vessel radii throughout the tree. The process of updating the radii after the new terminal segment is added will be from now on called *balancing of the tree*. Numerical implementation of this procedure is greatly facilitated by using the *bifurcation ratios* (e.g. ratios of segment radius to the radius of parent segment) instead of the actual radii. The whole subtree described by the bifurcation ratios can be scaled very easily.

The location of the start point of the new vessel is then optimized. As we recall it is first set to be an arbitrary point along the parent segment of the newly inserted terminal segment (midpoint of this segment in the implementation developed by the present author). The optimization aims at establishing the start point of the new segment, that minimizes the overall blood volume in the tree. The optimization procedure is described here in

a 2D setting. If we denote the blood volume in the entire tree as a function of start point of a new segment as $\mathcal{B}(x, y)$ the optimization proceeds as follows:

(i) estimate the size of the spatial step of the optimization Δl by taking it to be the smallest of the following numbers: 30% length of the new segment, 30% length of its sibling and difference in their lengths (provided it is nonzero),

(ii) calculate $\mathcal{B}(x, y)$, $\mathcal{B}(x + \Delta l, y)$ and $\mathcal{B}(x, y + \Delta l)$ (should any of these points be outside the tissue domain, then the sign of Δl is reversed),

(iii) the start point of the new segment is then moved in the direction of lowering $\mathcal{B}$, the spatial step is reduced and the procedure starting at step (ii) is repeated until $\mathcal{B}$ does not change significantly with each new iteration or maximum iteration number is exceeded.

It is worth noticing, that each evaluation of the function $\mathcal{B}(x, y)$ requires that the tree is rebalanced, ensuring that bifurcation rule holds and the hydraulic balance is preserved throughout the tree.

3.2.2. Determining the location of end point of new terminal segment. We return presently to the description of algorithm for adding the new terminal vessel into the tree (step 4 of the generation algorithm). Step (4.1) of that procedure consists of finding the location for the prospective new terminal segment. To this end a semi-random procedure is employed. It can be briefly described as follows:

(i) choose a random location P inside the region of interest,

(ii) calculate the minimum distance between P and every segment in the tree,

(iii) if the above-calculated distance falls below a prescribed threshold ϵ_R the procedure is repeated from step (i); if the number of repetitions exceeds a prescribed threshold, then ϵ_R is lowered by a constant ratio and the sequence is started afresh,

(iv) if the prospective location is sufficiently distant to each segment in the tree, it is accepted.

It should be remarked that the presented algorithm offers several possibilities for further improvements and extensions. These can be exploited to enable modelling of the features of real biological tissues. Let us describe two such potential directions of improvement.

The vasculature in living tissue is seldom homogenous on a large scale. Fatty tissue is relatively poorly vascularized, the blood circulation system of muscles is more developed and some internal organs have very complex and dense vascularity (e.g. liver or kidney). The possible way to model these inhomogeneities is to prescribe a nonhomogeneous probability density function which favours areas of higher tissue perfusion during the procedure of selection of an end point of the prospective new terminal vessel. The threshold ϵ_R can also be assigned different values for different tissues.

The other idea is to allow the threshold ϵ_R to be function of spatial variable. In this way, in certain areas, smaller distances between the segments would be allowed, while, in others, larger clearance between segments would have to be preserved.

3.2.3. Determining the parent segment for the new terminal segment. To complete the description procedure we now describe the algorithm for selecting the parent segment of the new terminal segment. It is the most time-consuming and—at the same time—probably the simplest part of the segment addition algorithm. The new terminal segment is added to each existing tree segment as its daughter segment in a manner described in Sec. 3.2.1. The total tree blood volume is calculated and the new terminal segment is removed. Finally the segment yielding the lowest blood volume is selected to be the parent for a new terminal segment.

It is worth noticing that each action of adding of the terminal segment involves numerous iterations of geometric optimization of the start point location procedure and the segment removal from the tree requires rebalancing of the tree. Furthermore, the selection algorithm slows down dramatically, as the number of segments in the tree increases.

For these reasons, the present author has proposed an improvement to the above-described procedure (which, in its general form, has been described in [10]). Instead of verifying suitability of every segment in the tree in the role of parent segment of the new terminal, only the one closest to the new terminal end point is tried, as well as only those others, whose distance to this point does not exceed twice the distance to the closest one. Then, the usual

procedure selects the one that yields the lowest blood volume in the tree. This improvement will be called the *preselection* in the following discussion.

The preselection narrows the search considerably and the procedure does not slow down very much with increasing number of segments in the tree. The reason for this behaviour is that, for any given point there is usually the same number of segments that are within twice the distance to the one closest to this point.

3.3. Example Results of Tree Generation

The described algorithm has been implemented in the form of the `grower` program. In the present version the program handles only two-dimensional, rectangular tissue regions. However, in principle, there are no significant obstacles to extending the functionality to other, convex 2D domains. The present author believes also, contrary to the opinion expressed by authors of [10], that the extension of the presented algorithm to nonconvex and three-dimensional domains is also possible.

3.3.1. Influence of geometric optimization and effectiveness of preselection procedure. Figure 3 presents the 101- and 301-terminal trees generated with optimization of the new terminal start-point (geometric optimization) turned on and off. In the non-optimized trees, not only the new segment is always inserted in the midpoint of the parent segment, but also the process of selecting the parent segment is conducted by means of comparison of the blood volumes in various non-optimized potential new trees. The results clearly do not resemble vascular trees. However, one must bear in mind that the geometrical optimization is the most time-consuming element of the algorithm. In Table 2 the times of tree generation with optimization turned on and off are compared for two trees (101 and 301 terminal segments). As one can see, including optimization slows the generation process considerably.

TABLE 2. Time (in seconds) of generation of 100 and 300 new terminals in the 2D vascular tree consisting initially of one segment. The generated trees are presented in Fig. 3.

number of terminals	no optimization no preselection	optimization no preselection	no optimization preselection	optimization preselection
100	4	121	<1	6
300	193	4773	5	86

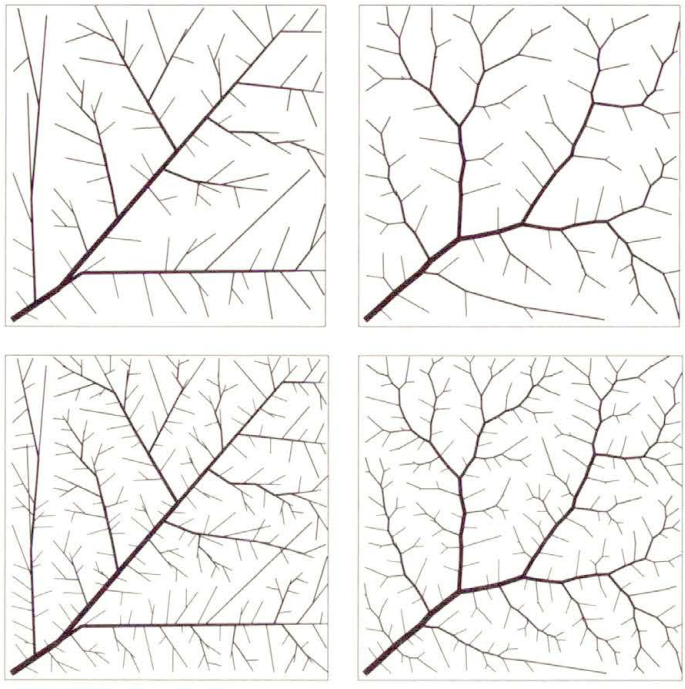

FIGURE 3. The trees generated with geometric optimization turned off (left) and on (right). Top: trees containing 101 terminal segments, bottom: trees with 301 terminal segments.

Table 2 gives also some idea about the effectiveness of the innovation introduced by the present author to the parent segment selection algorithm (preselection). Since the number of the potential possibilities to verify, in each segment addition step, does not grow significantly with the tree complexity, the preselection gives much smaller generation times, when compared to the full search. The generation rate does not drop so dramatically when the preselection method is used, which enables one to generate larger trees, such as the one presented in Fig. 4. The generation time of this tree was below sixty hours on 3 GHz PC. Without the preselection procedure, the generation of this tree would not be possible.

Also it should be remarked that the comparison of total blood volume in the generated trees was found to yield exactly the same value for trees generated with and without the preselection algorithm. It confirms the assumption that none of the potential parent vessels eliminated by preselection would have been selected by the full search procedure. For example the 301-terminal tree depicted in Fig. 3, bottom, right contains 32.2923 mm^3 of

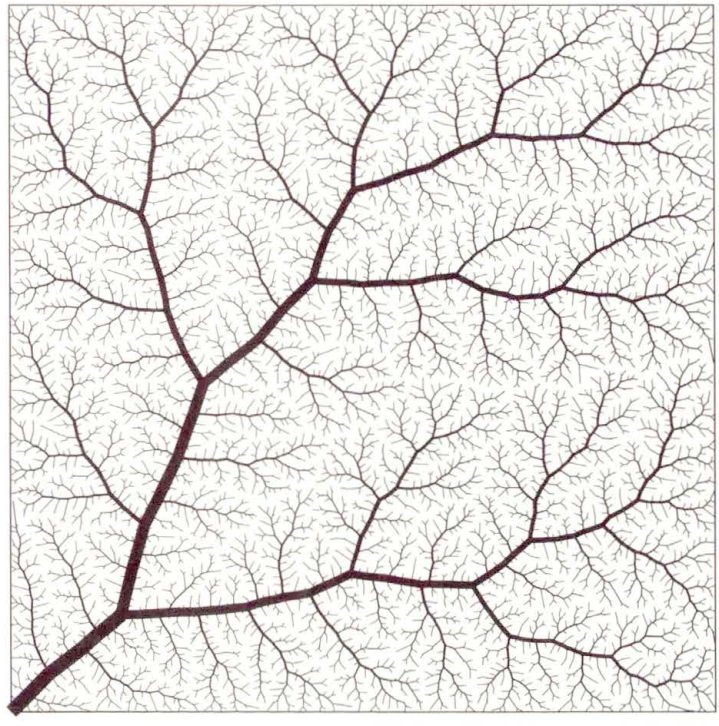

FIGURE 4. The tree containing 6000 terminal segments, generated using the geometric optimization and preselection procedures. The generation time was below 60 hours on 3 GHz PC.

blood and is generated during well over one hour by full search procedure. The preselection yields exactly the same volume, after almost one and a half of a minute. The verification of the blood volumes between the two methods was not tried for larger trees because the time necessary for a full search becomes excessive[1)].

3.3.2. Influence of the bifurcation exponent. The bifurcation exponent γ, introduced in Eq. (3.1) is a purely empirical parameter, estimated to be equal 2.7 for normal circulation system. However, it can be varied in the relatively wide range, yielding distorted vascular trees. Comparison of a number of results obtained for various values of γ are depicted in Fig. 5.

[1)] As the tree generation involves a random element, one would expect that the volumes of two 301-terminal trees would never be precisely equal. However quasi-random procedure employed in the actual implementation uses a random number generator that yields always the same sequence of pseudo-random numbers, which facilitates comparisons.

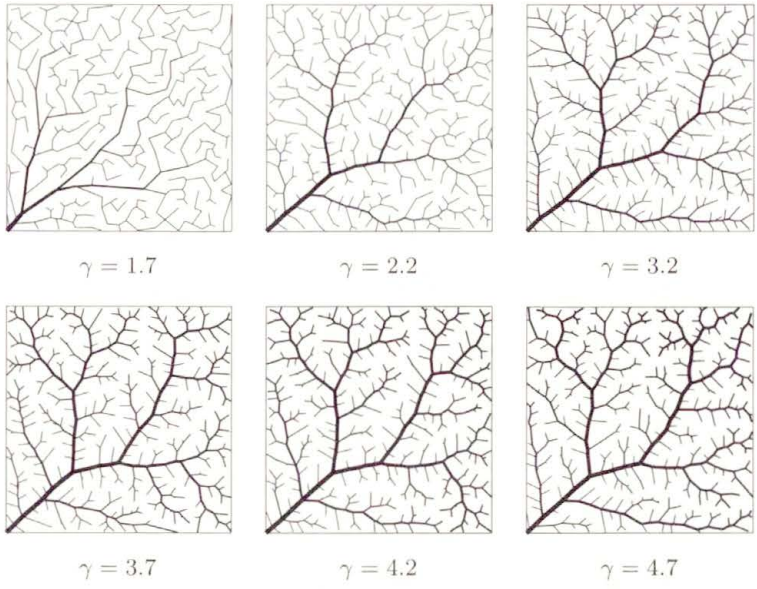

FIGURE 5. The 301-terminal trees generated using various non-standard values of the bifurcation exponent γ. The corresponding tree, generated with $\gamma = 2.7$ is depicted in Fig. 3, bottom, right.

4. Mesh and Grid Creation

Once the description of the vascular tree embedded in the tissue region of interest is available, the next step is to create discretization (mesh) of the tissue matrix and develop such spatial discretization of the vascular tree, that would be compatible with that mesh, i.e. that would facilitate the calculation of the coupled tissue and blood temperature problems. In practice, the mesh of the tissue domain has to be created and then the vascular tree is subdivided in such a way, that each tree segment can be assigned to a single element of tissue discretization (e.g. finite element). Usually, the tree is no longer a binary tree after such subdivision (parent segments are created, that have a single daughter segment).

A tissue domain mesh can be created by any method. It would probably be advantageous to devise method for simultaneous tissue domain mesh creation and vascular tree subdivision. That would allow one to control the size of the resulting tree segments and tissue elements. In the implementation employed in the `grower` program a simpler technique is adopted. The 2D rectangular tissue domain is subdivided into a prescribed number of elements and then, the vascular tree is subdivided.

The subdivided vascular tree and meshed tissue domain are called the *grid* in the following text. Each segment in the grid is embedded entirely in a single tissue domain element, and each element is assigned a list of segments embedded in it. In this way, the subsequent calculation of the heat exchange between the vascular tree and the tissue domain is greatly facilitated.

Apart from establishing a direct relation between the tissue domain and the vascular tree, the process of creating the grid allows one to calculate a number of parameters. These are:

- the number of segments per element,
- the number of terminal segments per element,
- blood fraction in the element.

Distribution of these parameters, calculated for the sparse grid, is depicted in the Fig. 6. The shades of gray in the figure are used to denote the absolute value of the blood fraction (white= 100%, black= 0%) or, for other parameters, the value relative to the maximum attained in the grid (white=maximum, black=0).

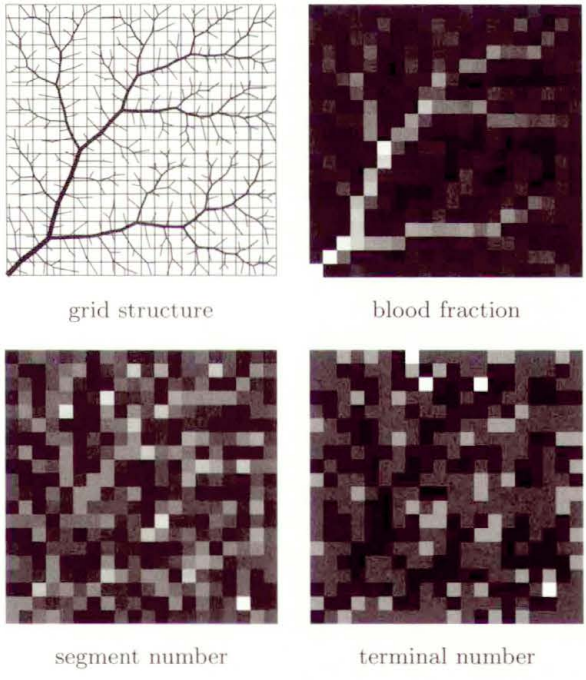

FIGURE 6. The grid created out of 301-terminal tree and a 20×20 mesh.

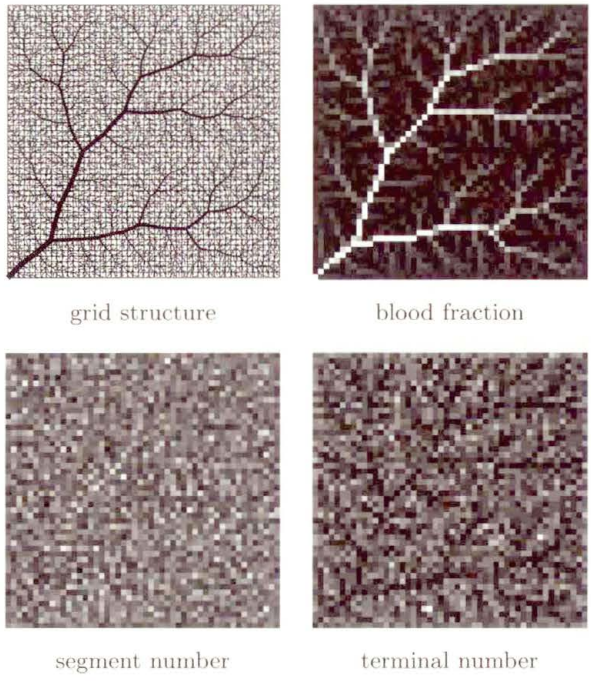

FIGURE 7. The grid created out of 7201-terminal tree and a 50×50 mesh.

The tree in Fig. 6 features 301 terminal segments and the number of segments before subdivision was 601 (the number of segments in any binary tree is twice the number of its terminals minus one). The tree was subjected to further division to match the tissue region mesh of 20×20 elements. After the subdivision the number of segments was 1137.

The example of a relatively complex grid is presented in the Fig. 7. The initial number of terminals was 7201 (14 401 segments) and, after division suitable for 50×50 mesh of tissue domain, the number of segments increased to 20 894.

5. Blood Temperature Calculations

5.1. Introduction

In the present section the geometrical model of the vasculature and tissue, whose generation and preparation has been described in the preceding sections, is used for calculation of the blood and tissue temperatures and heat fluxes.

As we recall, the vascular system is described by means of the complex tree of simple blood vessel pairs (segments). The tree is embedded in the surrounding tissue. A single vessel pair consists of artery and vein of circular cross-sections, lying in countercurrent arrangement. Apart from geometrical data, such as vessel radius r (common to both vessels and assumed constant throughout the length of the vessel), starting and ending points, the pair is characterized by the two temperatures (of arterial and venous blood): $T_{\mathrm{a}}(s)$ and $T_{\mathrm{v}}(s)$ respectively, that are dependent on the axial coordinate of the pair s, and by the blood velocity, that is assumed constant throughout the vessel. The tissue temperature along the vessel is denoted $T_{\mathrm{t}}(s)$. Figure 8 depicts the single segment.

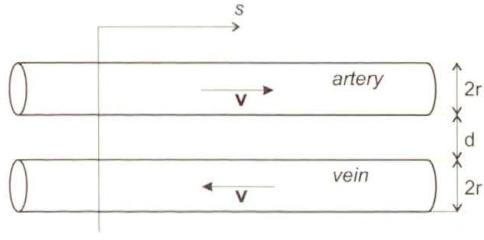

FIGURE 8. Primitive building block of vascular tree: countercurrent vessel pair segment

The condition of constant blood velocity along each segment corresponds to the assumption that no mass transfer takes place through the vessel walls. It may seem that this assumption excludes the phenomenon of the so-called large vessel bleed-off from considerations using the presented method. In fact, the present model allows very small vessels to branch off the large ones, and the flow through these very small vessels can be regarded as the model of bleed-off effect. In the opinion of the author, it is a valid, albeit numerically expensive, method of modelling the large-vessel bleed-off effect.

In the presented method, employed in the `flower` program (bottom in Fig. 1), the vessels are treated as one-dimensional entities immersed in the space of higher dimension (two or three). Therefore, whenever reference is made to vessel (arterial/venous) temperature, it is understood that the mixing-cup temperature is meant. The spatial variable for the vessel (axial coordinate) is denoted s.

5.2. Single Vessel Equilibrium

The considerations similar to those presented here can be found in [2, 1]. Let us consider the energy balance equation for the single vessel, embedded in medium, subject to heat flux along its length as depicted in Fig. 9.

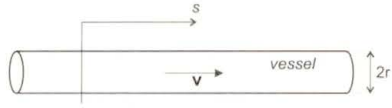

FIGURE 9. Single vessel embedded in medium

The energy balance equation reads:

$$\pi r^2 \frac{\partial E(s)}{\partial t} = 2\pi r q_{\mathrm{w}}(s) - \pi r^2 \frac{\partial q(s)}{\partial s} - \pi r^2 \rho_{\mathrm{bl}} c_{\mathrm{bl}} v \frac{\partial T(s)}{\partial s} \tag{5.1}$$

where $q_{\mathrm{w}}(s)$ denotes the heat flux received through the vessel wall, $q(s)$ is the conduction heat flux in the vessel and ρ_{bl} and c_{bl} are the density and specific heat of the fluid (blood) respectively.

In most physiological situations, the axial conduction in the blood can be neglected, also the internal energy of the blood can be expressed in terms of the temperature. Also the heat exchange through the vessel wall can be described by $\bar{q}_{\mathrm{w}}(s) = 2\pi r q_{\mathrm{w}}(s)$, a quantity of heat exchanged by the unit length of the vessel in unit time.

$$\rho_{\mathrm{bl}} c_{\mathrm{bl}} \frac{\partial T(s)}{\partial t} = \frac{1}{\pi r^2} \bar{q}_{\mathrm{w}}(s) - \rho_{\mathrm{bl}} c_{\mathrm{bl}} v \frac{\partial T(s)}{\partial s} \tag{5.2}$$

The heat flux received by the unit length of the vessel wall at s can be conceptually divided into two portions: the one received from the counter-current vessel q_{cc} and the one received from the surrounding tissue q_{t}. The former is proportional to the temperature difference between the vessels and to the conductivity of the tissue. The latter is proportional to the temperature difference between the vessel and the tissue and the conductivity of the tissue. Formally one has:

$$\bar{q}_{\mathrm{cc}} = \bar{\sigma}_{\mathrm{cc}} \lambda_{\mathrm{t}} (T_{\mathrm{cc}}(s) - T(s)), \tag{5.3}$$

$$\bar{q}_{\mathrm{t}} = \bar{\sigma}_{\mathrm{t}} \lambda_{\mathrm{t}} (T_{\mathrm{t}}(s) - T(s)), \tag{5.4}$$

$$\bar{q}_{\mathrm{w}} = \bar{q}_{\mathrm{cc}} + \bar{q}_{\mathrm{t}}. \tag{5.5}$$

Here $\bar{\sigma}_{cc}$ and $\bar{\sigma}_t$ are constant, dimensionless, shape coefficients for heat conduction between the vessels and between the vessel and the tissue respectively. They are assumed to depend on the geometry of the system only (vessel radius and spacing between vessels). A number of dimensional shape factors, determined for various geometries are given in [8]. For two parallel cylinders of diameters D_1 and D_2, lying a distance w apart (w is measured axis-to-axis) Incropera and DeWitt propose the following expression for the shape factor:

$$\bar{\sigma} = \frac{2\pi}{\cosh^{-1}\left(\frac{4w^2 - D_1^2 - D_2^2}{2D_1 D_2}\right)}.$$

For the cylinders of the same diameter $D_1 = D_2 = D$ lying two diameters apart $w = 2D$ one has:

$$\bar{\sigma} = \frac{2\pi}{\cosh^{-1}(7)} = \frac{2\pi}{\ln(7 + \sqrt{48})} \approx 2.3855.$$

For convenience of notation, we introduce shape coefficients per unit cross-sectional area of the vessel:

$$\sigma_{cc} = \frac{\bar{\sigma}_{cc}}{\pi r^2}; \qquad \sigma_t = \frac{\bar{\sigma}_t}{\pi r^2}.$$

5.3. Equilibrium of the Vessel Pair

We assume that the s-axis (axis of the vessel) is oriented in the direction of the blood flow in the artery and opposite to the flow in vein. We then have for the artery (for convenience, the dependence on s is not indicated):

$$\rho_{bl} c_{bl} \frac{\partial T_a}{\partial t} = \sigma_{cc}\lambda_t(T_v - T_a) + \sigma_t\lambda_t(T_t - T_a) - \rho_{bl} c_{bl} v \frac{\partial T_a}{\partial s}. \tag{5.6}$$

The corresponding equation for the vein is:

$$\rho_{bl} c_{bl} \frac{\partial T_v}{\partial t} = \sigma_{cc}\lambda_t(T_a - T_v) + \sigma_t\lambda_t(T_t - T_v) + \rho_{bl} c_{bl} v \frac{\partial T_v}{\partial s}. \tag{5.7}$$

The heat transported into tissue from the unit length of the vessel pair is therefore:

$$q_l = -\sigma_t\lambda_t((T_t - T_a) + (T_t - T_v)) = 2\sigma_t\lambda_t\left(\frac{T_a + T_v}{2} - T_t\right). \tag{5.8}$$

5.4. Numerical Formulation

We now reformulate the heat transfer problem in the framework of finite differences. Since each vessel pair segment is connected on one side to the parent segment, and on the other, it feeds one or two daughter segments it is convenient to consider a single vessel pair segment to be basic unit of the discretization. In the following derivations we denote the length of the segment by L, the time step of the simulation by Δt; the values at the start and end of the segment are denoted by superscript s and e. Spatial derivatives are calculated by forward-difference for vein and by backward-difference for artery. The reason for this choice is clarified below. The temperature gradients in both vessels of the pair are approximated to be constant throughout the segment.

5.4.1. Explicit Method In the explicit formulation all heat flow rates are calculated using the blood temperature values at the beginning of the time step. This method is significantly cheaper numerically, although it imposes severe limitation on the size of time step used. The artery and vein temperatures in segments are calculated sequentially, in the selected order.

Equation (5.6), yields the following algebraic equation for the end-segment temperature of arterial blood:

$$T_{\mathrm{a}}^{e}(t+\Delta t) = T_{\mathrm{a}}^{e}(t) + \Delta t \left(\frac{\lambda_{\mathrm{t}}}{\rho_{\mathrm{bl}} c_{\mathrm{bl}}} \left(\sigma_{\mathrm{cc}} (T_{\mathrm{v}}^{e}(t) - T_{\mathrm{a}}^{e}(t)) + \sigma_{\mathrm{t}} (T_{\mathrm{t}}^{e}(t) - T_{\mathrm{a}}^{e}(t)) \right) - v \frac{T_{\mathrm{a}}^{e}(t) - T_{\mathrm{a}}^{s}(t)}{L} \right). \tag{5.9}$$

Similarly, equation (5.7), yields the following algebraic equation for the start-segment temperature of venous blood:

$$T_{\mathrm{v}}^{s}(t+\Delta t) = T_{\mathrm{v}}^{s}(t) + \Delta t \left(\frac{\lambda_{\mathrm{t}}}{\rho_{\mathrm{bl}} c_{\mathrm{bl}}} \left(\sigma_{\mathrm{cc}} (T_{\mathrm{a}}^{s}(t) - T_{\mathrm{v}}^{s}(t)) + \sigma_{\mathrm{t}} (T_{\mathrm{t}}^{s}(t) - T_{\mathrm{v}}^{s}(t)) \right) + v \frac{T_{\mathrm{v}}^{e}(t) - T_{\mathrm{v}}^{s}(t)}{L} \right). \tag{5.10}$$

The chosen method for spatial gradient approximation requires that additional equations for the start-segment artery temperature and end-segment vein temperature are specified to complete the formulation. These equations

are simply *the mixing conditions* expressing the fact, that there is no accumulation of energy at the junctions between segments. The mixing condition for artery expresses the fact that the blood entering daughter vessels has the end-segment arterial temperature of the parent segment:

$$T_{\mathrm{a}}^{s}(t+\Delta t)=\begin{cases} T_{\mathrm{supply}} & \text{for root segment,} \\ \mathcal{P}\left(T_{\mathrm{a}}^{e}(t+\Delta t)\right) & \text{for non-root segment.} \end{cases} \tag{5.11}$$

Here T_{supply} is the prescribed arterial supply temperature, i.e. the temperature of the blood entering the arterial circulation in the considered tissue region; the operator $\mathcal{P}$ returns value of its argument for the parent of the considered segment (i.e. while $T_{\mathrm{a}}^{s}(t)$ denotes the segment start-point arterial temperature at time t, $\mathcal{P}(T_{\mathrm{a}}^{s}(t))$ denotes the segment start-point arterial temperature of the parent of the present segment at time t). We recall that there is only one segment (root segment) in the vascular tree that has no parent segment.

The mixing condition for venous blood expresses the fact that the end-segment temperature of the venous blood can be calculated as a result of mixing of two venous blood flows from the daughter segments:

$$T_{\mathrm{v}}^{e}(t+\Delta t)=\begin{cases} T_{\mathrm{t}} & \text{for terminal segment,} \\ \frac{1}{vr^2}\sum_{i=0}^{d}\mathcal{D}_i(vr^2 T_{\mathrm{v}}^{s}(t+\Delta t)) & \text{for non-terminal segment.} \end{cases} \tag{5.12}$$

Here we denote by d the number of daughter segments to the considered segment and introduce the operator $\mathcal{D}_i$ that refers to the variables of the ith daughter segment of the considered segment. This operator is analogous to $\mathcal{P}$. We recall that the segments having no daughter segments are referred to as *terminal segments*. In the model it is assumed that the blood in terminal segments is in thermal equilibrium with surrounding tissue and therefore any blood draining into venular vessels of those segments is at the local tissue temperature.

For stability of the presented numerical scheme for the artery (5.9), the following condition must hold:

$$\Delta t<\left(\frac{\lambda_{\mathrm{t}}}{\rho_{\mathrm{bl}}c_{\mathrm{bl}}}(\sigma_{\mathrm{cc}}+\sigma_{\mathrm{t}})+\frac{v}{L}\right)^{-1}. \tag{5.13}$$

It can be readily verified that the formulation for vein (5.10) yields an identical criterion. Since the first term in the parenthesis on the r.h.s. of (5.13)

is of several orders of magnitude smaller than the second term, one can infer that the condition pertinent to the blood advection determines stability.

Unfortunately, the brief inspection of the grid creation method described in the Sec. 4 shows that the vascular tree segments can get arbitrarily small in the course of subdivision. There are two kinds of situations, where such unusually short vessels arise. They are schematically depicted in Fig. 10.

Due to these anomalous tree segments the direct application of the explicit method is untenable. The calculation of the shortest segment length for the sparse grid in Fig. 6 and dense grid in Fig. 7 yielded the lengths of the order of 10^{-6} and 10^{-9} m respectively. Calculation of the maximum time step ensuring stability of the numerical formulation, according to Eq. (5.13) resulted in times of the order 10^{-10} and 10^{-13} s respectively. Clearly these values are too small for simulation.

Three solutions to this problem can be proposed:

- preconditioning of the grid prior to calculations (see middle rectangle in Fig. 2); The shortest vessel segments can be eliminated by appropriate repositioning of the nodes of the tissue region mesh and—possibly—by slight corrections of the shape of the tree. Using the latter method, one needs to ensure that the hydraulic balance and the bifurcation rule are not violated, also the changes of the shape of the tree have to be very small so that the optimality ensured by the growth algorithm is not disturbed much. These two approaches are illustrated in Fig. 11. The

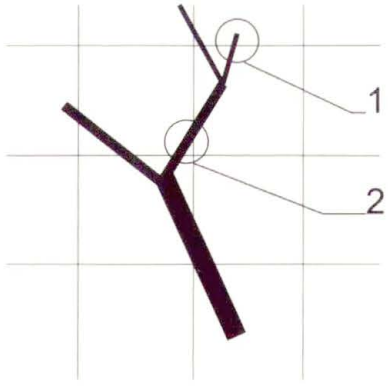

FIGURE 10. Two kinds of situation, where arbitrarily short segments arise in subdivision during the creation of the grid: 1. segment traverses the mesh element boundary with its end-point very close to this boundary; 2. segment traverses the mesh element very close to its corner.

drawback of this method is the fact that the appropriate algorithm for repositioning the tissue region mesh nodes seems to be rather difficult to devise.

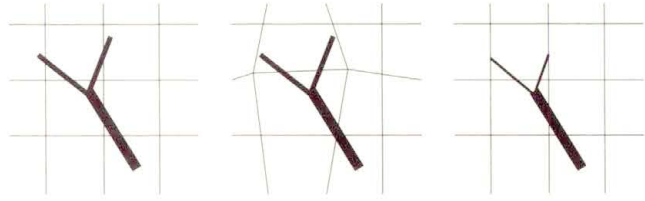

FIGURE 11. Two ways of improving an initial grid (a), which contains two very short terminal segments. In (b) the tissue region mesh is deformed and in (c) the vascular tree is truncated, the vessel radii being adjusted to obey the bifurcation rule and hydraulic balance law.

- omitting the shortest segments in the numerical formulation; If the shortest segment is the only daughter segment of its parent or is a parent to only one daughter segment (most of the shortest segments are expected to fall in that category), then it can be treated together with its parent (daughter) segment as a single segment in the numerical scheme. All heat exchanged with the tissue elements would be distributed between the tissue elements surrounding the segments according to the lengths ratio of the segments. This situation is schematically depicted in Fig. 12.
- application of the numerical scheme that imposes no limit (such as Eq. (5.13)) on the time step used, e.g. implicit finite differences method. This method will be discussed in the next subsection.

5.4.2. Implicit method. In the implicit method, the artery and vein temperatures in segments are calculated simultaneously. The tissue temperatures are still calculated separately so heat flow rates are calculated on the basis of the blood temperatures at the end of the current step and current (start of the step) tissue temperatures. The method requires solving the appropriate system of equations, whose size is determined by the number of segments. It is unconditionally stable, so a time step size larger than the one used in explicit formulation may be selected.

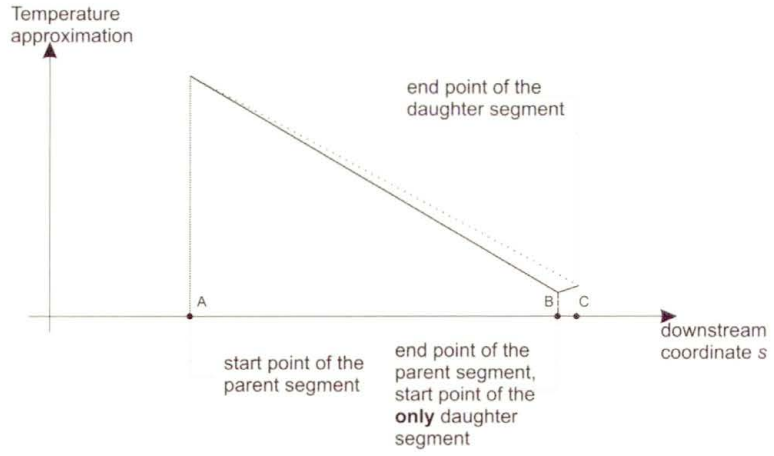

FIGURE 12. In the numerical scheme, treating the parent-single daughter succession of segments as a single segment means that the intermediate node will be omitted and the approximation of the temperature will be the one denoted with dotted line as opposed to the example of original one (solid line). In this example, the parent segment AB lies within the element I of tissue domain mesh, while its only daughter vessel—in the element II. The heat exchanged by the combined segment AC with the tissue is split between the elements I and II in proportion to the lengths AB and BC. Temperatures at nodes A, B, and C are set arbitrarily in this example.

Equation (5.6), yields the following algebraic equation for the end-segment temperature of arterial blood:

$$T_{\mathrm{a}}^{e}(t+\Delta t)\left(1+\Delta t\left(\frac{\lambda_{\mathrm{t}}\sigma_{\mathrm{cc}}}{\rho_{\mathrm{bl}}c_{\mathrm{bl}}}+\frac{v}{L}\right)\right)-T_{\mathrm{v}}^{e}(t+\Delta t)\left(\frac{\lambda_{\mathrm{t}}\sigma_{\mathrm{cc}}\Delta t}{\rho_{\mathrm{bl}}c_{\mathrm{bl}}}\right)$$
$$-T_{\mathrm{a}}^{s}(t+\Delta t)\frac{v\Delta t}{L}=T_{\mathrm{a}}^{e}(t)+\frac{\lambda_{\mathrm{t}}\sigma_{\mathrm{t}}\Delta t}{\rho_{\mathrm{bl}}c_{\mathrm{bl}}}\left(T_{\mathrm{t}}^{e}(t)-T_{\mathrm{a}}^{e}(t)\right). \quad (5.14)$$

Similarly, equation (5.7), yields the following algebraic equation for the start-segment temperature of venous blood:

$$T_{\mathrm{v}}^{s}(t+\Delta t)\left(1+\Delta t\left(\frac{\lambda_{\mathrm{t}}\sigma_{\mathrm{cc}}}{\rho_{\mathrm{bl}}c_{\mathrm{bl}}}+\frac{v}{L}\right)\right)-T_{\mathrm{a}}^{s}(t+\Delta t)\frac{\lambda_{\mathrm{t}}\sigma_{\mathrm{cc}}\Delta t}{\rho_{\mathrm{bl}}c_{\mathrm{bl}}}$$
$$-T_{\mathrm{v}}^{e}(t+\Delta t)\frac{v\Delta t}{L}=T_{\mathrm{v}}^{s}(t)+\frac{\lambda_{\mathrm{t}}\sigma_{\mathrm{t}}\Delta t}{\rho_{\mathrm{bl}}c_{\mathrm{bl}}}\left(T_{\mathrm{t}}^{s}(t)-T_{\mathrm{v}}^{s}(t)\right). \quad (5.15)$$

Equations (5.11) and (5.12) hold also in the case of the implicit method.

5.4.3. Summary The pair of equations (5.9) and (5.10), or (5.14) and (5.15), along with (5.11), and (5.12) enable the calculation of arterial and venous temperatures at time $t + \Delta t$. The tissue temperature is calculated independently, by means of the suitable numerical procedure for integration of nonstationary heat conduction equation. Each segment of the vascular tree embedded in the tissue provides local line heat source of intensity described by Eq. (5.8). Furthermore, each terminal segment provides point heat source of intensity

$$q_{\text{term}} = \pi r^2 \rho_{\text{bl}} c_{\text{bl}} v (T_{\text{a}}^e - T_{\text{v}}^e), \tag{5.16}$$

located at its end-point. It should be noted that the vascular tree embedded in the tissue domain of interest, should be sufficiently complex (the vasculature should be modeled to a sufficient level of detail), so that the blood reaching terminal vessels is in thermal equilibrium with tissue and q_{term} is small. In real organisms the artery-vein connection takes place at the level of capillaries, where the blood is in full equilibrium with the tissue, even on the most extreme thermal loadings. In most cases, the temperature equilibrating takes place several branching generations earlier, cf. [7].

5.4.4. Implementation of the Implicit Method In order to implement the above-mentioned finite difference scheme an appropriate numbering is adopted. Each tree segment is assigned a number i being an integer multiple of 3, so that the segments are indexed with the numbers $0, 3, 6, \ldots$ The following degrees of freedom are then introduced for each segment:

number	meaning
0	T_{a}^e
1	T_{v}^s
2	T_{v}^e

The global number of the degree of freedom is then obtained by adding the local number of the degree of freedom to the segment number. For example the end-of-segment venous temperature in the segment 21 (that is the eight segment) will be denoted θ^{23} (21 for segment and 2 for T_{v}^e).

The start-of-segment arterial temperature need not to be treated as an unknown variable, since, by Eq. (5.11) it can be replaced by appropriate parent segment temperature, therefore we have three temperature degrees of freedom per segment.

Before the matrix form of the implicit method is derived we introduce some convenient notations:

$$\alpha = \frac{\lambda_{\mathrm{t}} \Delta t}{\rho_{\mathrm{bl}} c_{\mathrm{bl}}}, \qquad \beta^n = \frac{v(n)\Delta t}{L(n)}$$

where the variable n denotes the segment number, e.g. $v(n)$ is the blood velocity in the nth segment. Furthermore, by $T_{\mathrm{t}}^{n,s}$ we denote tissue temperature at the location of start-point of the n-th segment while by $T_{\mathrm{t}}^{n,e}$ we denote tissue temperature at the location of end-point of the n-th segment.

The global matrix for nodal temperature calculation is constructed by inserting three equations for every segment in the tree. That is, for every segment n we proceed as follows:

1. if the segment n is a root segment:

   (a) enter the following equation no. n into the constructed system:

$$\theta^n(t+\Delta t)(1+\alpha\sigma_{\mathrm{cc}}+\beta^n) - \theta^{n+2}(t+\Delta t)\alpha\sigma_{\mathrm{cc}} = \theta^n(t)(1-\alpha\sigma_{\mathrm{t}}) + \alpha\sigma_{\mathrm{t}} T_{\mathrm{t}}^{n,e}(t) + T_{\mathrm{supply}}\beta^n,$$

   (b) enter the following equation no. $n+1$ into the constructed system:

$$\theta^{n+1}(t+\Delta t)(1+\alpha\sigma_{\mathrm{cc}}+\beta^n) - \theta^{n+2}(t+\Delta t)\beta^n = \theta^{n+1}(t)(1-\alpha\sigma_{\mathrm{t}}) + \alpha\sigma_{\mathrm{t}} T_{\mathrm{t}}^{n,s}(t) + T_{\mathrm{supply}}\alpha\sigma_{\mathrm{cc}},$$

2. if the segment n is not a root segment:

   (a) determine the number m of the parent segment of n,

   (b) enter the following equation no. n into the constructed system:

$$\theta^n(t+\Delta t)(1+\alpha\sigma_{\mathrm{cc}}+\beta^n) - \theta^{n+2}(t+\Delta t)\alpha\sigma_{\mathrm{cc}} - \theta^m(t+\Delta t)\beta^n = \theta^n(t)(1-\alpha\sigma_{\mathrm{t}}) + \alpha\sigma_{\mathrm{t}} T_{\mathrm{t}}^{n,e}(t),$$

   (c) enter the following equation no. $n+1$ into the constructed system:

$$\theta^{n+1}(t+\Delta t)(1+\alpha\sigma_{\mathrm{cc}}+\beta^n) - \theta^m(t+\Delta t)\alpha\sigma_{\mathrm{cc}} - \theta^{n+2}(t+\Delta t)\beta^n = \theta^{n+1}(t)(1-\alpha\sigma_{\mathrm{t}}) + \alpha\sigma_{\mathrm{t}} T_{\mathrm{t}}^{n,s}(t),$$

3. determine numbers of the daughter segments p and o (or just p if there is only one daughter segment),

4. if there are no daughter segments (n is a terminal segment) enter the following equation no. $n+2$ into the constructed system,

$$\theta^{n+2}(t+\Delta t) = T_{\mathrm{t}}^{n,e}(t)$$

5. if there is one daughter segment p of the segment n enter the following equation no. $n+2$ into the constructed system

$$\theta^{n+2}(t+\Delta t) - \theta^{p+1}(t+\Delta t) = 0,$$

6. if there are two daughter segments p and o of the segment n enter the following equation no. $n+2$ into the constructed system

$$v(n)r^2(n)\theta^{n+2}(t+\Delta t) - v(p)r^2(p)\theta^{p+1}(t+\Delta t) - v(o)r^2(o)\theta^{o+1}(t+\Delta t) = 0.$$

In the resulting set of equations the equation having the same number k as some segment corresponds to Eq. (5.14) for that segment, equation with number $k+1$ corresponds to Eq. (5.15) for that segment and equation numbered $k+2$ corresponds to the mixing condition Eq. (5.12) for that segment. Temperature continuity condition for that segment Eq. (5.11) is already used in the formulation (three temperature DOFs per segment instead of four).

6. Tissue Temperature Calculations

For the calculations of tissue temperature the usual Fourier-Kirchhoff conduction equation is used:

$$\rho_{\mathrm{t}} c_{\mathrm{t}} \phi_{\mathrm{t}} \frac{\partial T_{\mathrm{t}}}{\partial t} = \lambda_{\mathrm{t}} \nabla^2 T_{\mathrm{t}} + q_{\mathrm{m}} + q_{\mathrm{bl}}. \tag{6.1}$$

Here q_{m} is a constant metabolic volumetric heat source, while ϕ_{t} is the local volumetric tissue fraction and q_{bl} is the net heat exchanged by the tissue with the blood vessels per tissue element volume. Its calculation procedure is described in the following.

Equation (6.1) is solved numerically using the finite element method for discretization in space and finite difference method for time discretization. The vascular tree model is subdivided as described in Sec. 4, so that each segment of the tree is contained in a single tissue element. In other words, each tissue element k can be assigned a set of n_k tree segments located inside it and a set of m_k terminals located inside it (obviously $n_k \geq m_k$). It is

pointed out that the tissue fraction ϕ_t can be readily calculated (see Figs. 6 and 7) and remains constant in time (unless one takes the thermoregulation effects into account).

The blood-flow-related volumetric heat source q_{bl} is calculated for each element and is subdivided in two components:

$$q_{bl}^{(k)} = \frac{1}{V^{(k)}} \left(\hat{q}_l^{(k)} + \hat{q}_{term}^{(k)} \right). \tag{6.2}$$

Here $V^{(k)}$ is the volume of the kth element, $\hat{q}_l^{(k)}$ is the heat conducted from the walls of all vessels embedded in the kth element to the tissue matrix (see Eq. (5.8)), and $\hat{q}_{term}^{(k)}$ is the heat transported at the tips of all the terminal vessels embedded in the kth element to the tissue matrix (this heat accounts for the possible temperature difference between arterial end-of-terminal temperature and the end-of-terminal venous temperature, see Eq. (5.16)). The first term in parentheses in Eq. (6.2) is calculated as follows (see Eq. (5.8)):

$$\hat{q}_l^{(k)} = 2\sigma_t \lambda_t \sum_{i=1}^{n_k} \int_{start(i)}^{end(i)} \left(\frac{T_a(l) + T_v(l)}{2} - T_t(l) \right) dl \tag{6.3}$$

where start(i) and end(i) denote the starting and ending point of the ith segment contained within the considered element, l being the local coordinate of the segment.

The second term in parentheses in Eq. (6.2) is obtained (see Eq. (5.16)):

$$\hat{q}_{term}^{(k)} = \pi \rho_{bl} c_{bl} \sum_{i=1}^{m_k} r^2(i) v(i) (T_a^e - T_t). \tag{6.4}$$

In the course of numerical calculations all temperatures on the r.h.s. of Eqs. (6.3, 6.4) are taken from the previous time step (explicit formulation).

7. Example Results—Steady-state Temperature Distribution

The presented method was implemented in a computer program and used in a number of example simulations. Here we pass to the description of the selected results. The simulations were done on the moderately dense grid consisting a vascular tree comprising of 301 terminals (601 segments, 1137 segments after tree meshing) and 20×20 tissue mesh (441 nodes). The linear dimension of the region was 22.31 mm. The setup is depicted in Fig. 13.

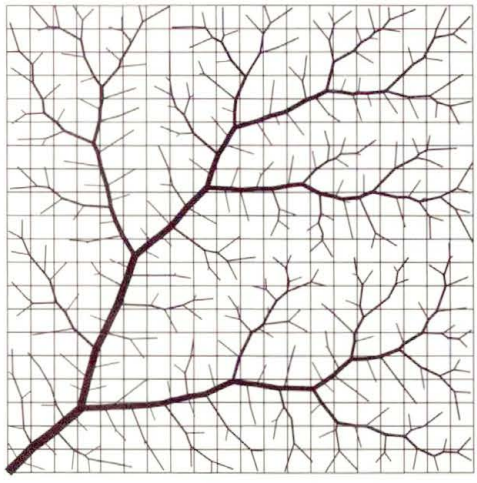

FIGURE 13. Vascular tree model and tissue mesh used in the calculations

Since no thermoregulatory loop was introduced (blood flow is independent of temperature), the hydraulic calculations were performed just once, at the beginning of the simulation.

For the simulation adiabatic boundary conditions were assumed on lower, left and right boundaries of the tissue region. The top boundary was maintained at 25°C. The initial tissue temperature was assumed to be 25°C. The blood feeding the system via arterial vessel of the root segment was kept at 37°C. Obviously, the return blood temperature in the root was calculated by the model. The metabolic heat generation rate was set to be $7000\,\mathrm{W/m^3}$.

The steady-state was obtained by computing subsequent steps of time-transient simulation until temperatures did no longer change.

Figure 14 displays the calculated temperature of the blood particle as it traverses the region of interest, starting in the arterial vessel of the root segment, making its way to the most distant terminal in the tree, and, after entering the venous circulation, returning to the draining vessel of the root segment. The scale on the horizontal axis is in arbitrary units (1 corresponds to the width (height) of the square domain of interest).

The data in Fig. 14 have clear physical interpretation. The warm blood, perfusing cool region of tissue gets cooler as it flows through arterial part of the tree. The temperature variations are continuous. At the furthest point of the selected circulation loop (at the end of the terminal vessel) the blood attains the local body temperature, which happens to be 25.25°C (the terminal

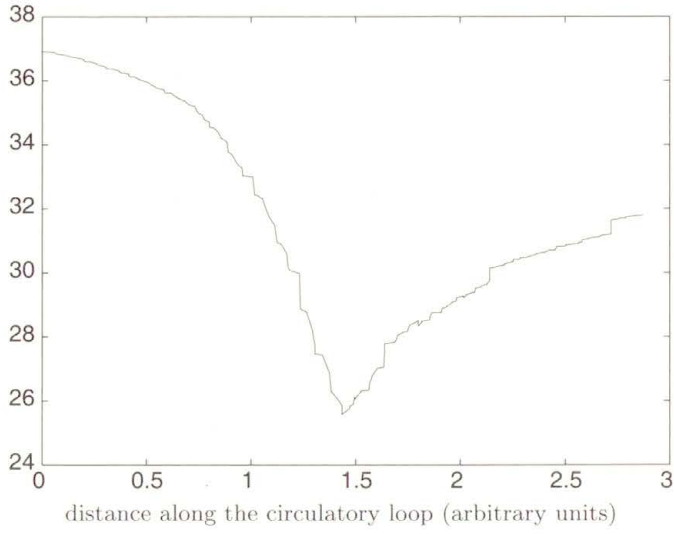

FIGURE 14. Blood temperature along the circulation path feeding the terminal most distant to the root segment; Horizontal axis corresponds to the length (in arbitrary units) along that path.

lies close to the isothermal outer boundary, kept at 25°C). The blood then enters the venous circulation and travels towards the root. On its way it is rewarmed by the counter-current artery and its temperature rises. The process is discontinuous in this case as the blood streams mix in every junction. Finally the root segment is reached, the return venous temperature being ca. 31.8°C.

Since the temperature in the venous tree is discontinuous through the branchings, the vessel-to-vessel heat flow and consequently the slope of the arterial temperature curve can also be expected to be discontinuous. Indeed—careful inspection of Fig. 14 reveals that there are no discontinuities on the arterial side, although the slope is sometimes very high. Summarizing: the temperature curve of the arterial circulation continuous but nonsmooth due to discontinuous vessel-to-vessel heat flux. The vessel-to-vessel flux is, in turn, discontinuous due to venous blood temperature jumps at branchings where mixing takes place. This feature of the model is a consequence of assumption that blood mixing in the branchings of the venous circulation is immediate.

It is noteworthy that the rough scheme in Fig. 1 and the calculated results of the model, presented in Fig. 14 are similar.

The steady-state averaged temperature distribution in the vertical direction is presented in Fig. 15.

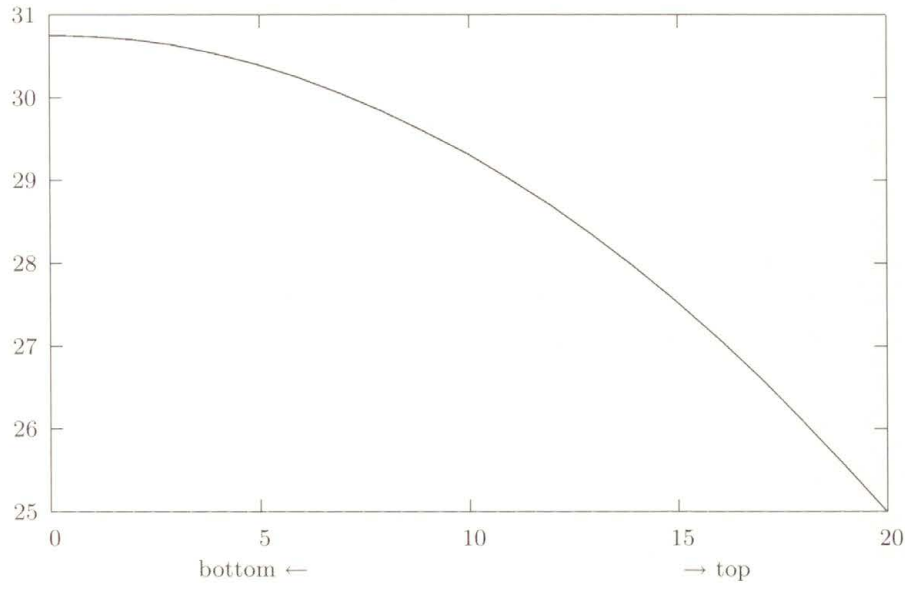

FIGURE 15. Horizontally-averaged tissue temperature profile.

8. Conclusions

The presented method allows one to take account of the impact of countercurrent blood flow through the vascular tree of prescribed geometry on the heat transfer in soft tissue. It uses three independent temperatures: arterial blood temperature, venous blood temperature, and tissue temperature. Therefore, no simplifying assumptions regarding the relation between these are needed (in contrast to e.g. model presented in [15]). This advantage is attained at the expense of model complication and numerical cost of the calculations.

Possibly the most serious limitation of the presented results is the fact that they were obtained with a 2D implementation. Extension to fully three-dimensional case is required if clinically-relevant calculations are to be attempted. It should be pointed out that the method is not intrinsically two-dimensional and the 2D implementation developed to obtain results presented here was chosen on the basis of its simplicity and clarity of presentation.

The presented method is well suited to the investigation of thermoregulation phenomena. It is known that, among other mechanisms of thermoreg-

ulation, the vasodilation and vasoconstriction plays a prominent role. For that purpose the model needs to be supplemented with the additional law relating the relative vessel radius to the local temperature. The pressure/flow calculation is then performed at every step of time-transient analysis.

Nonhomogeneously-perfused tissues can be described by the presented model as well. The vascular tree generation algorithm can be adjusted to yield small vessel density in some tissue regions (e.g. adipose tissue) and large vessel density in the others, for example by introducing a spatial variation of probability density for growing a new terminal. It should be remarked however that for clinically-applicable simulations of effect of large vessels on local hyperthermia, use of real, measured vessel geometry would probably be better [14].

Acknowledgement

The presented work was financially supported by the Ministry of Science and Information Technology (Poland), grant No. 4 T11F 003 25.

References

1. J.W. BAISH, P.S. AYYASWAMY, and K.R. FOSTER, *Small-scale temperature fluctuations in perfused tissue during local hyperthermia*, J. Biomech. Eng. **108**: 246–250, 1986

2. J.W. BAISH, P.S. AYYASWAMY, and K.R. FOSTER, *Heat transport mechanisms in vascular tissues: a model comparison*, J. Biomech. Eng. **108**: 324–331, 1986

3. A. BEJAN, *From heat transfer principles to shape and structure in nature: constructal theory*, J. Heat Transfer, **122**: 430–449, 2000

4. A. BEJAN, *The tree of convective heat streams: its thermal insulation function and the predicted 3/4-power relation between body heat loss and body size*, J. Heat Mass Transfer, **44**: 699–704, 2001

5. H. BRINCK and J. WERNER, *Estimation of the thermal effect of blood flow in a branching countercurrent network using a three-dimensional vascular model*, J. Biomech. Eng. **116**: 324–330, 1994

6. C.K. CHARNY, S. WEINBAUM, and R.L. LEVIN, *An evaluation of the Weinbaum-Jiji bioheat equation for normal and hyperthermic conditions*, J. Biomech. Eng. **112**: 80–87, 1990

7. M.M. CHEN and K.R. HOLMES, *Microvascular contributions in tissue heat transfer*, Annals New York Acad. Sci. **335**: 137–154, 1980

8. F.D. INCROPERA and D.P. DEWITT, *Fundamentals of Heat and Mass Transfer 4th. ed.* John Wiley&Sons New York, Chichester, Brisbane, Toronto, Singapore 1996

9. H.H. PENNES, *Analysis of tissue and arterial blood temperatures in the resting human forearm*, J. Appl. Physiology **1** : 93–122, 1948

10. W. SCHREINER and P.F. BUXBAUM, *Computer-optimization of vascular trees*, IEEE Trans. BME **40**(5) : 482–491, 1993

11. T.F. SHERMAN, *On connecting large vessels to small: the meaning of Murray's law*, J. Gen. Physiol., **78** : 431–453, 1981

12. M. STAŃCZYK and J.J. TELEGA, *Modelling of heat transfer in biomechanics—a review. Part I. Soft tissues*, Acta Bioengng. Biomech. **4**(1) : 31–61, 2002

13. L.A. TABER, S. NG, A.M. QUESNEL, J. WHATMAN and C.J. CARMEN, *Investigating Murray's law in the chick embryo*, J. Biomech., **34** : 121–124, 2001

14. G.M.J. VAN LEEUWEN and A.A. VAN STEENHOVEN, *Heat Transfer in Humans—Local and Whole-Body*, Abiomed Lecture Notes **6**, Blood Flow Modelling and Diagnostics, T.A. Kowalewski [ed.], Warsaw 2005.

15. S. WEINBAUM and L.M. JIJI, *A new simplified bioheat equation for the effect of blood flow on local average tissue temperature*, J. Biomech. Eng. **107** : 131–139, 1985

16. S. WEINBAUM, L.M. JIJI, and D.E. LEMONS, *The bleed-off perfusion term in the Weinbaum-Jiji bioheat equation*, J. Biomech. Eng. **114** : 539–544, 1992

17. G.B. WEST, *The origin of universal scaling laws in biology*, Physica A, **263** : 104–113.

18. E.H. WISSLER, *Pennes' 1948 paper revisited*, J. Appl. Physiology **85**(1) : 35–41, 1998

19. W. WULFF, *The energy conservation equation for living tissue*, IEEE Trans. BME **21**(6) : 494–495, 1974